Influence of microorganisms on uranium release from mining-impacted lake sediments under various oxygenation conditions

Marina Seder-Colomina, Arnaud Mangeret, Pascale Bauda, Jessica Brest, Lucie Stetten, Pauline Merrot, Anthony Julien, Olivier Diez, Evelyne Barker, Elise Billoir, et al.

Influence of microorganisms on uranium release from mining-impacted lake sediments under various oxygenation conditions

Marina Seder-Colomina[a], Arnaud Mangeret[a,*], Pascale Bauda[b], Jessica Brest[c], Lucie Stetten[a,c], Pauline Merrot[c], Anthony Julien[a], Olivier Diez[a], Evelyne Barker[a], , Elise Billoir[b], Pascal Poupin[b], Antoine Thouvenot[d], Charlotte Cazala[a], Guillaume Morin[c]

[a]Institut de Radioprotection et de Sûreté Nucléaire (IRSN), PSE-ENV/SEDRE, 31 avenue de la Division Leclerc, 92260 Fontenay-aux-Roses, France.

[b]Université de Lorraine, CNRS, LIEC, F-57000 Metz, France

[c]Institut de Minéralogie, de Physique des Matériaux et de Cosmochimie (IMPMC), UMR 7590 CNRS-Sorbonne Université -MNHN-IRD, case 115, 4 place Jussieu, 75252 Paris Cedex 5, France

[d]Athos Environnement, 63171 Aubière, France

To be submitted to Environmental Science: Processes & Impacts

*Corresponding author: arnaud.mangeret@irsn.fr

Tel +33 1 58 35 76 95

Fax +33 1 46 57 62 58

ABSTRACT

Microbial processes can be involved in the remobilization of uranium (U) from reduced sediments under O_2 reoxidation events such as water table fluctuations. Such reactions could be typically encountered after U-bearing sediment dredging operations. Solid U(IV) species may thus reoxidize into U(VI) that can be released in pore waters in the form of aqueous complexes with organic and inorganic ligands. Non-uraninite U(IV) species may be especially sensitive to reoxidation and remobilization processes. Nevertheless, little is known regarding the role of microbially mediated processes on the behaviour of U under these conditions.

In this study, laboratory incubation experiments were performed, under three different oxygenation conditions (0, 50 and 100% O_2-saturation, referred to as oxic, hypoxic and anoxic). The incubation experiments were conducted on fresh sediments from Lake Saint-Clement formely impacted by U mining activities, and containing ~300 mg/kg of U, mainly under the form of mononuclear U(IV) species (60-80%). XANES analysis of the incubated sediments shows that U(IV) was fully oxidized to U(VI) under oxic and hypoxic conditions and remained U(IV) under anoxic conditions. Nevertheless, hypoxic conditions lead to the lowest U release in solution after three weeks (3.6 $\mu g.L^{-1}$), whereas oxic and anoxic conditions slightly favored U release (8.3 – 15.5 $\mu g.L^{-1}$, respectively). Geochemical modeling suggested that U was mainly released as aqueous U(VI)-carbonate and Ca-U(VI)-carbonate complexes under oxic/hypoxic and anoxic conditions, respectively. Semi-confined hypoxic conditions were found to stimulate microbial Fe^{2+} oxidation, which lowers the pH, limits U complexation to bicarbonate ions and potentially produces ferric-oxyhydroxides able to sorb U(VI). Molecular analyses yield genomic evidence for an increasing abundance of Fe oxidizers under these conditions and thus support their possible role in decreasing U mobility.

1. INTRODUCTION

Uranium (U) is one of the most common and persistent subsurface contaminants from the front end of the nuclear cycle, such as former U mining activities; notably due to its long half-life of 4.4 billion years and its chemical and radiological toxicities to human beings and biota [1]. In France, the extraction of U by open-pit and underground mining has concerned approximately 250 sites, from 1948 to 2001 [2]. After their closure, U mine wastes, including mill tailings, waste rocks and mining-impacted soils and sediments, constitute a potential source of radionuclides to surface environments, which need to be appropriately monitored and managed through time. Several studies have shown that U can accumulate in reducing environments such as wetlands [3-7], alluvial aquifers [8] and lake sediments [9-10] downstream from U mining and processing sites. In France, lake and pond sediments that have been significantly enriched in U because of former U mining activities can be allowed to be dredged and stored in a surface storage site. Depending on the physico-chemical conditions these operations could potentially induce transformations of the U redox state and mobility in sediments [11]. Moreover, little is known regarding the potential effect of these treatments on microbial activities, especially if these sediments were anoxic prior to dredging operations.

The long-term efficiency of U retention in sediments is largely controlled by the nature of the U chemical species [12-13], pH and redox regimes [14]. The presence of organic [15-16] and inorganic carbon [11,17] as well as other inorganic ligands [18] is also an important factor to consider. Notably U(VI) is known to form highly mobile stable complexes with carbonates such as $UO_2(CO_3)_2^{2-}$, conversely to sparingly soluble U(IV) species [19]. In addition, biological activity can directly or indirectly modify U speciation and significantly lower U mobility[19]. For instance, enzymatic microbial reduction of U(VI) can directly lead to the formation of low-soluble U(IV) species [21-22]. Moreover, indirect reduction of U(VI) to U(IV) can be favoured by

72 Fe(II)-rich phases such as bio-reduced phyllosilicates [10,23] or green rusts [24]. On the contrary it
73 has been shown that under slightly acidic laboratory conditions Fe(III)-bearing minerals may
74 reoxidize bio-uranitite or biogenic U(IV) with a release of dissolved Fe(II) [25-26]. Microbial
75 alkaline phosphatase activity may also induce periplasmic precipitation of U(VI)-phosphate
76 minerals[27]. Finally, biosorption to bacterial surfaces and exopolymers [28-30] as well as to
77 mineralized cells and biofilms [30-33] are also important U scavenging mechanisms.
78 Lake Saint-Clément, situated in the Massif-Central (France) is an artificial reservoir
79 impacted by discharges of treated U mine waters from the site of Bois-Noirs Limouzat [9].
80 Detailed geochemical and mineralogical analyses of well-preserved sediment cores from this
81 Lake [9-10] suggested that early diagenesis processes below the sediment-water interface lead to
82 the indirect reduction of U(VI) to mononuclear U(IV) species by Fe(II) produced from the
83 bioreduction of Fe(III)-rich chlorite, e. g. chamosite. In the same studies, X-ray absorption
84 spectroscopy of the samples indicated that these early-diagenetic U(IV) species were mostly
85 non-crystalline and consisted of sorbed mononuclear U(IV). A set of experiments was
86 previously conducted in order to investigate the sensitivity of these U(IV) species to reoxidation
87 [11]. This latter study indicated that oxidizing conditions slightly remobilized U after 8 days but
88 bicarbonate addition highly increased U remobilization, even under reducing conditions[11].
89 Despite these results yielded a first insight in the reactivity of these sediments, the possible role
90 of autochtonous microbial population on U(IV) remobilization processes was not investigated.
91 To date, the study of microbial cycling of U have been mostly focused on its interaction with
92 bacteria [34-35]. However, a recent study reported a bioassociation between U and archaea species
93 in rock salts in Germany [36]. Moreover, archaea species have already been identified nearby U
94 polluted sites [37]. Among prokaryotes, archaea species are considered non-negligible in various
95 environments, especially in soils and aquatic freshwater ecosystems, where they are estimated

to represent 2% [38] and 1% [39] of the microbial diversity, respectively. Their role on U reoxidation and especially upon reoxidation events by O_2 from fresh sediments is still largely unexplored.

The objective of the present study was to evaluate the influence of microbial communities on U reoxidation and mobilization from lake sediments during three-weeks long batch incubation experiments mimicking the first step of sediment dredging and surface storage operation. In the lake sediments studied, more than 85% of U is reduced in the form of mononuclear U(IV), which is representative of the speciation of U contaminated sediments [9,10,40,41,42]. Three different incubation conditions were investigated: full oxygenation that could occur under open-air surface repository conditions, anoxic conditions representing that would be expected under water-saturated conditions at the bottom of a storage pile, and 50% oxic conditions that may be the most relevant to storage sites. Our results indicate that intermediate oxidizing conditions (50% oxic) yielded the lowest U release rate even if mononuclear U(IV) was fully oxidized. According to the evolution of the physicochemical parameters of the incubation suspension (pH, alkalinity, $Fe^{2+}_{(aq)}$) and of microbial diversity, this results is interpreted as resulting from U(VI) scavenging by iron-oxyhydroxides resulting from microbial Fe(II) oxidation.

2. MATERIALS AND METHODS

2.1. Samples studied

Lake Saint Clément is located 20 km downstream from the former U mine of Bois Noirs/Limouzat in the Massif Central (France). It is supplied by the Besbre River, which is collecting the discharge of treated mine waters from the U mining site since its closure in 1980 (Figure S1). A sediment core of ~130-cm length was collected in August 2016 (46° 5' 9'' N, 3° 41' 22'' E) from a boat above the 12-meter-deep water column (at 120 meters upstream from the dam), using an Uwitec© gravity handcorer. Special care was given to the preservation of U

121 oxidation state by sealing the two core sections of 65-cm length into heat-sealed aluminized
122 plastic films bags within an N_2-filled anoxic glove bag on the field. Core sections were then
123 conditioned below 4°C for transportation to the laboratory where they were vacuum dried in an
124 N_2-filled anoxic glove box (<5 ppm O_2). A previous study of the Lake Saint Clément sediments
125 reported an increase of U concentration with depth, from 40 $mg.kg^{-1}$ at the top of the
126 sedimentary column to 360 $mg.kg^{-1}$ at 180-cm depth [9]. For this study, sediment samples
127 containing 195 to 233 $mg.kg^{-1}$ of U were selected from deep sediment layers, in which U is
128 mainly present as mononuclear U(IV) and minor amounts of nano-crystalline U(IV)-phosphate
129 [9]. These sediments are characterized by a high organic carbon content (8.5-12 wt% of total
130 organic carbon), constant Si (around 20 wt%) and P content (0.17 wt%), Fe from 4 to 6-8 wt%
131 and Ca from 0.37 to 0.55 wt% [10]. They mainly consists of quartz, feldspar, micas and chlorite,
132 with traces of barite and pyrite [9]. Concentrations of dissolved nitrate and sulfide concentration
133 in pore waters were below the detection limits of classical colorimetric methods suggesting that
134 sulfide and nitrate were not key compounds of the U redox cycle in the sediments studied [10].
135 For our experiments, lake waters sampled at 12 m depth, i.e. close to the sediment-water
136 interface, were collected using a Niskin bottle and used as incubation medium.
137

138 ## 2.2. Experimental setup

139 The Lake water was filtered through a 0.22-µm filter and O_2 was removed via N_2-bubbling
140 at 80°C during 1 hour. Once in a N_2-filled glove box, fresh anoxic sediments from the bottom
141 of the core (112-117 cm depth) were mixed with the anoxic lake waters at a solid:liquid ratio
142 of 1:10 under sterile conditions, using an electric burner. For each experimental condition,
143 approximately 66 g of the lake water/sediment suspension was poured into a sterile flask.
144 For differentiating abiotic and biotic effects on U mobility, all three oxygenation conditions
145 were performed either under biotic conditions using fresh sediments or under abiotic conditions

using sediments previously sterilized by gamma-irradiation as explained hereafter. Each condition was performed in triplicate. For abiotic experiments, the filled flasks were irradiated using a ^{60}Co sealed source at a total absorbed dose rate of 30 ± 1.68 kGy (1.5 kGy per hour) at the Ionisos irradiation facility in Dagneux, France. This mode of sterilization was considered successful, with no viable cells counted in gamma-sterilized sediments at a total gamma-ray dosage of 20 kGy [43].

Incubations were conducted at room temperature under three distinct O_2 conditions: fully oxic "*100% O_2*" Erlenmeyer flasks agitated at 300 rpm, hypoxic "*50% O_2*" Erlenmeyer flasks agitated at 10 rpm, and anoxic "*0% O_2*" Erlenmeyer flasks agitated at 300 rpm inside N_2-filled anoxic glove box Jacomex® GPT3 (> 5 ppm). For all experiments each Erlenmeyer was closed with a sterile, air-permeable, cotton stopper. Dissolved oxygen was monitored weekly using a Multi 350i Set WTW® probe during the experiment and values were 8.52 ± 0.23 and 4.62 ± 0.66 mg/L for the *100% O_2* and *50% O_2* experiments, respectively. For the *0% O_2* experiments, a value of $2.82.10^{-5} \pm 6.84.10^{-6}$ mg/L dissolved oxygen was calculated using Henry's law, based on the pO_2 value measured in the anoxic glovebox atmosphere.

Suspension samples taken at starting point (Time = 0) and after 1, 2, and 3 weeks of incubation were filtered through a 0.22-µm pore-size cellulose filter. Colorimetric analyses of alkalinity [44] and of dissolved Fe^{2+} and Fe^{3+} [45] were performed immediately after filtration. Acidified (pH~1, HNO_3) and non-acidified aliquots were also stored at 4°C for further analyses of dissolved cations and anions, respectively. Dissolved U was determined using an ICP-MS 8800 Triple Quadrupole (Agilent). Relative standard deviation was below 10% as estimated from 5 measurements of the same sample, and limit of quantification was 0.03 $\mu g.L^{-1}$. Dissolved major cations were measured using an ICP-OES iCAP™ 7600 Duo (Thermo Fisher Scientific). Relative standard deviation was below 10% as estimated from 5 measurements of the same sample, and detection limits were 10, 100, 40, 100 and 30 $\mu g.L^{-1}$ for Fe, Ca, K, P and Si,

171 respectively. Total Dissolved Carbon (DC) was determined by measuring the CO_2 released after
172 combustion at 850°C using a Carbon analyser (Vario TOC Cube analyzer, Elementar) equipped
173 with a non-dispersive infra-red detector. Dissolved Organic Carbon (DOC) was estimated as
174 DOC = DC - Alkalinity.
175 Starting sediment were analyzed as dry solid powders for Total Carbon (TC) using the same
176 method as above. Total Organic Carbon (TOC) was also determined using the same method but
177 the sample was acidified with a 1M HCl solution prior to combustion. The Total Inorganic
178 Carbon (TIC) was then deduced from the difference between TC and TOC. Relative standard
179 deviation was below 10% as estimated from 5 measurements of the same sample and limits of
180 quantification were 0.019 and 0.05 ppm for solid TC and TOC respectively and 0.5 ppm for
181 DOC.
182

183 ## 2.3. XAS spectroscopy

184 X-ray Absorption Near-Edge Structure Spectroscopy (XANES) was used to determine U
185 redox in the sediments before and after the incubation experiments. For this purpose, final solid
186 samples were harvested by centrifugation after 3 weeks of incubation and vacuum dried in an
187 N_2-filled anoxic glove-box. The collected sediments were vacuum dried in the same glove-box.
188 All samples were ground in an agate mortar, pressed as 7 mm diameter pellets sealed between
189 two layers of Kapton tape and mounted in Kapton-taped sample holders, in the same anoxic
190 glove-box. They were then transported to the synchrotron facility within aluminized foil bags
191 Protpack® sealed under anoxic atmosphere and placed into an anoxic plastic box containing a
192 GasPak™. The sample bags were opened in an anoxic glove box at the beamline and samples
193 were transferred inside the liquid N_2 cryostat, where they were placed under vacuum after N_2
194 purge of the sample chamber.
195 Eight samples were analyzed for XANES measurements at the U L_{III}-edge: 2 starting

196 samples (a non-irradiated and an irradiated fresh sediment) and 6 final samples, corresponding
197 to fresh and irradiated sediments incubated for 3 weeks under the 3 different oxygen conditions.
198 Data were collected in fluorescence detection mode using a 100-element solid state Ge array
199 fluorescence detector at the high-flux 11-2 wiggler beam line of the Stanford Synchrotron
200 Radiation Lightsource (SSRL, USA). The energy of the incident beam delivered by the Si(220)
201 double-crystal monochromator was calibrated by setting the first inflection point of Y *K*-edge
202 at 17038 eV, using a double transmission setup. Data were collected at 80K (liquid N_2 cryostat)
203 in order to avoid photoreduction of U(VI) under the X-ray beam [46]. A minimum of 2 scans were
204 collected for each sample, and series of up to 8 repeated scans on the same spot of selected
205 samples indicated no redox change of U under beam exposure. XANES data were merged and
206 normalized using the ATHENA code [47]. XANES spectra were fit using Linear Combination
207 Least Square (LC-LS) of the spectra of our purest U(IV) and U(VI) species, namely U(IV)-
208 citrate and U(VI)-pyrophosphate [9]. Using such a classical LC-LS procedure, determination of
209 the U(IV) and U(VI) proportions rely both on the energy-shift in L_3-edge position between the
210 two oxidation states (~2.7 eV) and on the characteristic shoulder in the XANES spectrum of
211 the uranyl ion $U^{VI}O_2^{2+}$ [6-11]. The fit were performed with a home-built code [9,48] based on
212 Levenberg-Marqardt minimization algorithm. The quality of the LC-LS fits was estimated by
213 a R-factor: $Rf = \Sigma [\mu_{exp} - \mu_{calc}]^2 / \Sigma \mu_{exp}^2$ where μ is the normalized absorbance. The uncertainty
214 on XANES LC-LS fitting components was estimated by $3 \times \sqrt{3 \sqrt{}}[VAR(p). \chi^2_R]$ (Ravel and
215 Newville, 2005), where $VAR(p)$ is the variance of component p for the lowest χ^2_R value; with
216 $\chi^2_R = N / (N-N_p) \sum [\mu_{exp} - \mu_{calc}]^2$, where N_p is the number of fitting components and N is the
217 number of independent parameters. N was calculated as the energy range divided by the natural
218 width of the U L_{III} [49].
219

2.4. Microbial analyses and bioinformatics

Total genomic DNA was extracted from 3 independent samples of fresh sediments in initial conditions as well as after 3 weeks incubation under contrasting oxygenation conditions (*0% O_2*, *50% O_2* and *100% O_2*). Amplicons of the V4 region were sequenced and a total of 9.070.946 paired-end reads (with a mean read length of 243 bases) were generated through Illumina MiSeq sequencing. Initial fresh sediments and those sampled after 3 weeks of incubation were separated by centrifugation (20 minutes at 6000 and 8500 rpm in the glove box and under oxidizing conditions respectively). DNA was extracted from pellets using the Powersoil DNA isolation kit Mobio on triplicate samples per incubation condition. Purified DNA was quantified by fluorescence using the Picogreen DNA quantification kit (Invitrogen). Libraries, sequencing and data analysis described in this section were performed by Microsynth AG (Balgach, Switzerland).

To sequence the V4 regions of the bacterial 16S rRNA gene, two-step Nextera PCR libraries using the primer pair 515F (5′-GTG CCA GCM GCC GCG GTA A -3′) and 806R (5′- GGA CTA CHV GGG TWT CTA AT-3′) were created [50]. Subsequently the Illumina MiSeq platform and a v2 500 cycles kit were used to sequence the PCR libraries. The produced paired-end reads which passed Illumina's chastity filter were subject to de-multiplexing and trimming of Illumina adaptor residuals using Illumina's real time analysis software included in the MiSeq reporter software v2.6 (no further refinement or selection). The quality of the reads was checked with the software FastQC version 0.11.7 [51]. The locus specific V4 primers were trimmed from the sequencing reads with the software cutadapt v1.18 [52]. Paired-end reads were discarded if the primer could not be trimmed. Trimmed forward and reverse reads of each paired-end read were merged to *in-silico* reform the sequenced molecule considering a minimum overlap of 15 bases using the software USEARCH version 11.0.667 [53]. Merged sequences were then quality

245 filtered allowing a maximum of one expected error per merged read. Reads that contain
246 ambiguous bases or are outliers regarding the amplicon size distribution are also discarded. The
247 remaining reads were denoised using the UNOISE algorithm implemented in USEARCH to
248 form operational taxonomic units (OTUs) discarding singletons and chimeras in the process.
249 The resulting OTU abundance table is then filtered for possible bleed-in contaminations using
250 the UNCROSS algorithm and abundances are adjusted for 16S copy numbers using the
251 UNBIAS algorithm. OTUs were compared against the reference sequences of the RDP 16S
252 database [54] and taxonomies were predicted considering a minimum confidence threshold of 0.7
253 using the SINTAX algorithm implemented in USEARCH. Alpha diversity was estimated using
254 the Richness (Observed), Chao1 and Shannon indexes. Beta diversity was calculated using the
255 weighted Unifrac distance method [55] on basis of rarefied OTU abundance counts per sample.
256 Alpha and beta diversity calculations and the rarefaction analysis were performed with the R
257 software packages phyloseq v1.22.3 and vegan v2.5-1. To detect differentially abundant OTUs
258 depending on collected sample metadata (e.g., medication, environmental conditions),
259 differential OTU analysis on normalized abundance counts was performed with the R software
260 package DESeq2 v1.18.1 [56].

261 To reveal inter-sample relations, non-metric multidimensional scaling (NMDS) based on the
262 Bray-Curtis dissimilarity (k=3) was performed. A permutational multivariate analysis of
263 variance (PERMANOVA) was also performed, with 999 permutations using the *adonis*
264 function of the *Vegan* R package.. Venn diagram and heat maps were produced using
265 respectively the *venn* and *heatmap.2* functions from the *gplots* R package [58]. The selection of
266 the 30 most abundant OTUs was based on raw abundances, whereas log10-transformed
267 abundances (log10(1+x)) are shown on heat maps. Sequences were registrated under accession
268 number PRJNA669547 in the SRA database of NCBI.

Richness and diversity estimates were calculated (Table S1). The Chao1 estimator indicated good coverage of OUT and richness throughout, and asymptotic rarefaction curves analysis for all samples (Figure S4) revealed that the overall prokaryotic diversity was well represented. Specific richness and evenness were expressed by the Shannon index. The highest diversity was observed in the initial sample, whereas incubation conditions reduced the diversity. *0% O_2* and *100% O_2* conditions revealed lower diversities, in contrast, the *50% O_2* condition presented the closest Shannon index value to the one observed in initial conditions (Table S1).

3. RESULTS

3.1. Evolution of solution chemistry in the incubation experiments

The chemical composition of the filtered supernatant solutions was followed over the course of the incubation experiments, by measuring dissolved U (Figure 1), pH and alkalinity (Figure 2), dissolved organic carbon (Figure S2) as well as total dissolved Fe and Fe^{2+}. (Figure 3). Other major elements including Ca, K, P and Si were also measured, as reported in Figure S3.

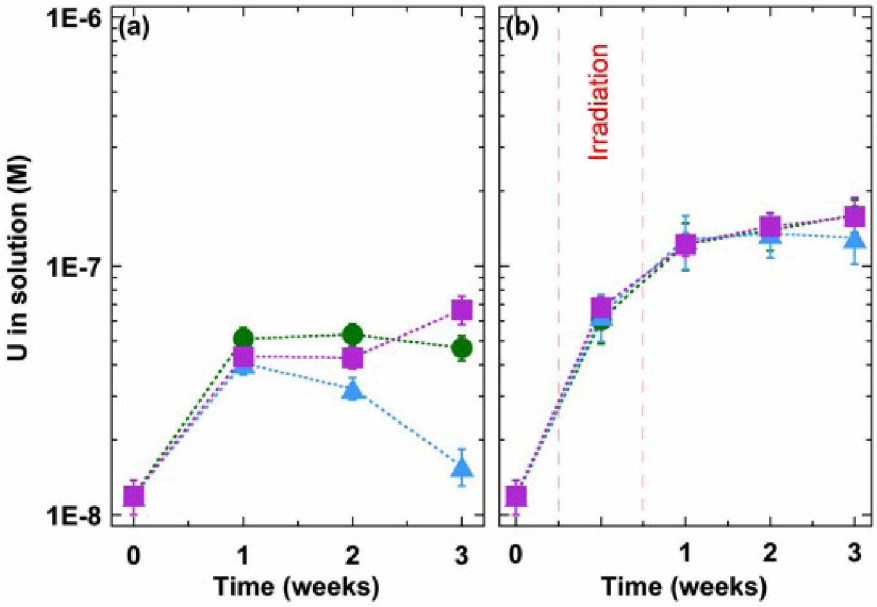

Fig. 1 Uranium mobilization for (a) non-irradiated and (b) irradiated sediments, throughout 3-week incubation under different O_2 conditions: ● *100% O_2* incubation; ▲ *50% O_2* incubation; (■, *0% O_2*. Error bars represent the standard deviation over the 3 replicates for each condition.

For the non-irradiated sediments (Figure 1a) the amount of dissolved U, released over time in the incubation supernatant differed with the oxygenation conditions, whereas it did not vary with the oxygenation conditions for the irradiated sediments (Figure 1b). More precisely, for the non-irradiated sediment (Figure 1a), under *100% O_2*, dissolved U increased and stabilized until the third week. Under *50% O_2*, U release was followed by a decrease in dissolved U concentration. Finally, under *0% O_2*, the release of U increased all along the experiment. For the irradiated sediments (Figure 1b), the dissolved U concentration increased over time, following a same pattern under the three oxygenation conditions, and the U release was overall higher than for the non-irradiated sediments.

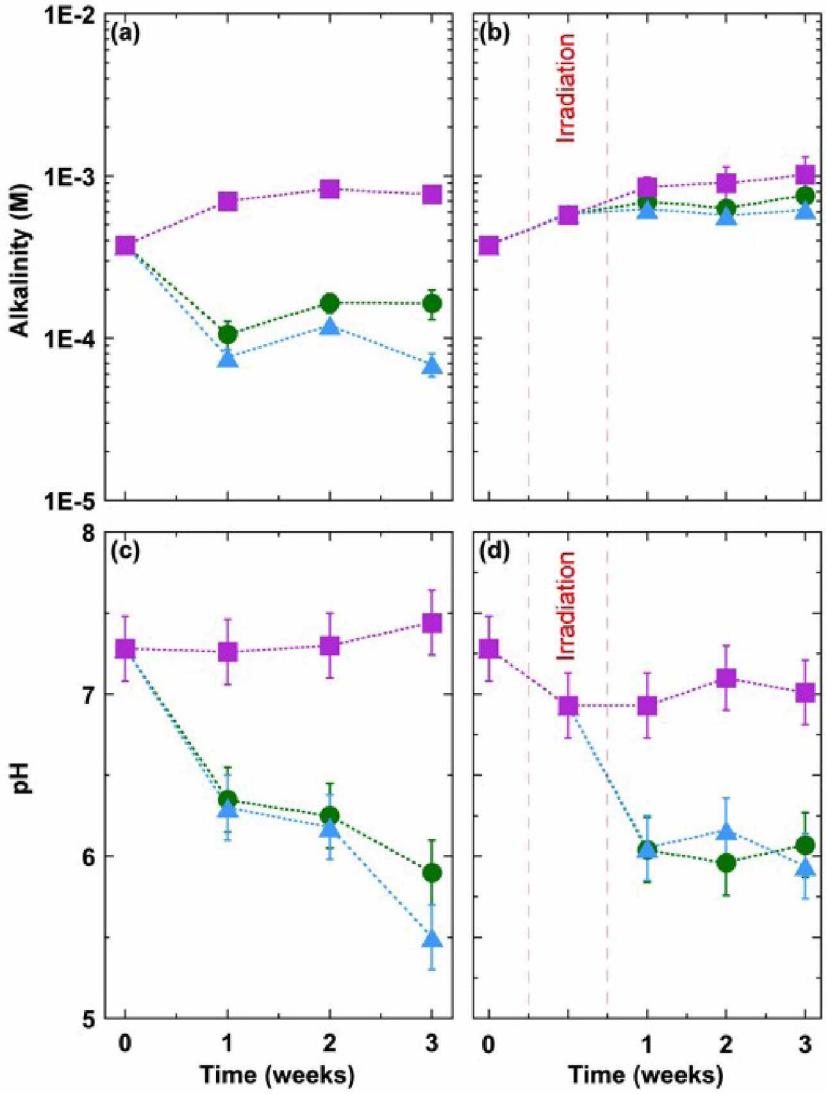

Fig. 2 Alkalinity and pH for (a, c) fresh and (b, d) irradiated sediments, throughout 3-week incubation under different O_2 conditions: ● *100% O_2* ; ▲ *50% O_2* ; ■ *0% O_2*. Error bars represent the standard deviation over the 3 replicates for each condition.

Alkalinity was found to increase with time in all experiments except in the *50% O_2* and *100% O_2* experiments conducted with the non-irradiated sediments (Figure 2a and b). The increase in alkalinity is interpreted as resulting from an increase in the buffering capacity of the solution, which could be explained by the progressive release of alkaline and alkaline-earth cations (Figure S3), as well as the release of aqueous Fe^{2+} (Figure 3a,b) in the anoxic incubations. The pH remained neutral under *0% O_2* conditions, whereas it significantly dropped over incubation time under *50 and 100% O_2* conditions (Figure 2 c,d), down to pH 5.5 for biotic *50% O_2*

312 conditions. Aqueous H_2CO_3 concentrations calculated from measured alkalinity and pH values
313 (Figure 2) were found to be in the range of $4.15\ 10^{-5}$ to $1.69\ 10^{-3}$ M, thus in excess with respect
314 to the value expected for equilibrium with atmospheric CO_2 ($[H_2CO_{3aq}] = 1.41\ 10^{-5}$M). This
315 result suggests that our incubation media did not fully degassed the CO_2 produced by the pH
316 drop, which could be related to the cotton stopper of the Erlenmeyer vessels that were used.
317 Interestingly, it is expected that the observed pH decrease (Fig. 2c,d) was caused by Fe(II)
318 oxidation under oxygenation conditions (Fig. 3). Under fully anoxic conditions (*0% O_2)*, total
319 dissolved Fe concentrations were the highest and Fe was mainly released in the first week of
320 incubation, essentially in the form of Fe(II), the same trend being observed for non-irradiated
321 and irradiated samples (Figure 3). In contrast, under *100% O_2* conditions, approximately half
322 of the initial dissolved Fe was progressively removed from the solution and this Fe removal
323 was even more pronounced under *50% O_2* conditions. Abiotic experiments exhibited a similar
324 behaviour but with less pronounced Fe removal under *50% O_2* conditions. The decrease of total
325 Fe observed in the presence of oxygen, can be partly explained by the removal of Fe(II) (Figure
326 3c,d), which suggests Fe(II) oxidation and subsequent precipitation of iron oxides, well known
327 as resulting in an acidification of the medium.

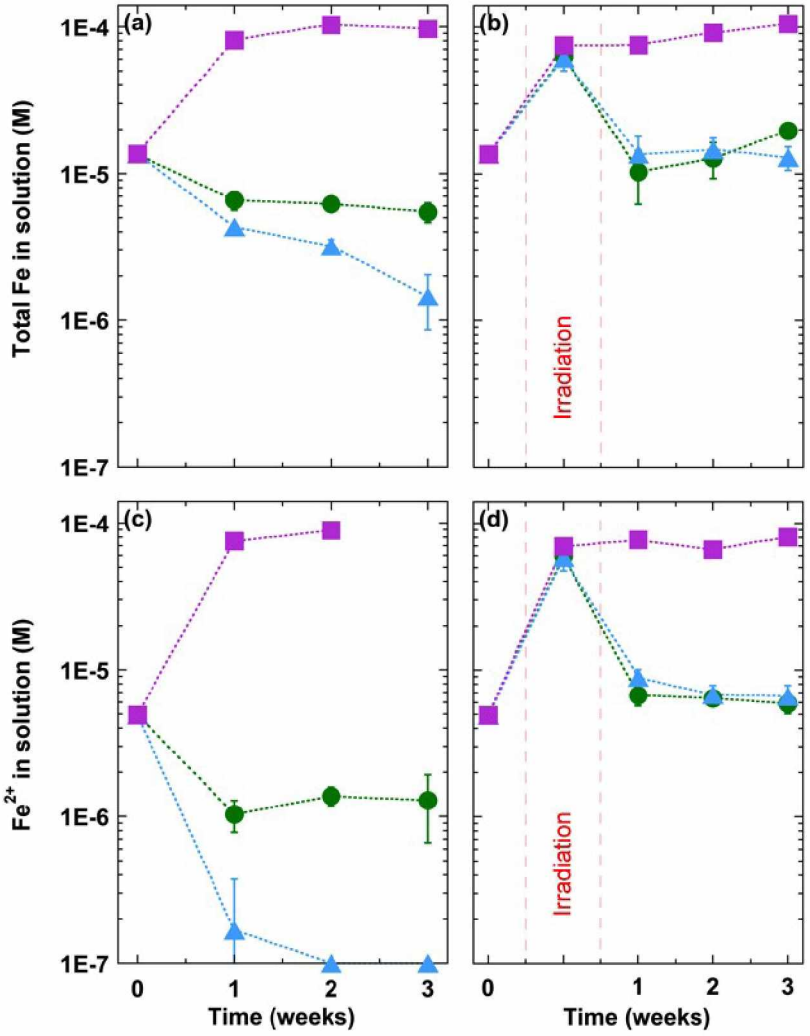

328

329 **Fig. 3** Total Iron in solution and Fe^{2+} in solution for (a, c) fresh and (b, d) irradiated sediments.
330 Measures during 3 weeks of incubation under different O_2 conditions: green circles (●), *100%*
331 *O_2* incubation; blue triangles (▲), *50% O_2* incubation and purple squares (■), *0% O_2* incubation.
332 Error bars represent the standard deviation over the 3 replicates for each condition.

333

334 The above-mentioned results regarding the solution chemistry led us to infer that
335 microaerophilic conditions are the most favourable conditions for decreasing U remobilization
336 from the lacustrine sediments. The removal of both dissolved U (Figure 1) and Fe(II) (Figure
337 3) under biotic hypoxic conditions especially suggested that Fe oxidation could have limited U
338 release under these conditions, which is further discussed thereafter.

339

3.2. Evolution of solid U oxidation state

U oxidation state was assessed using XANES spectroscopy in the solid phase of fresh and irradiated sediments at the start of the experiments and after 3 weeks of incubation (Figure 3; Table S2).

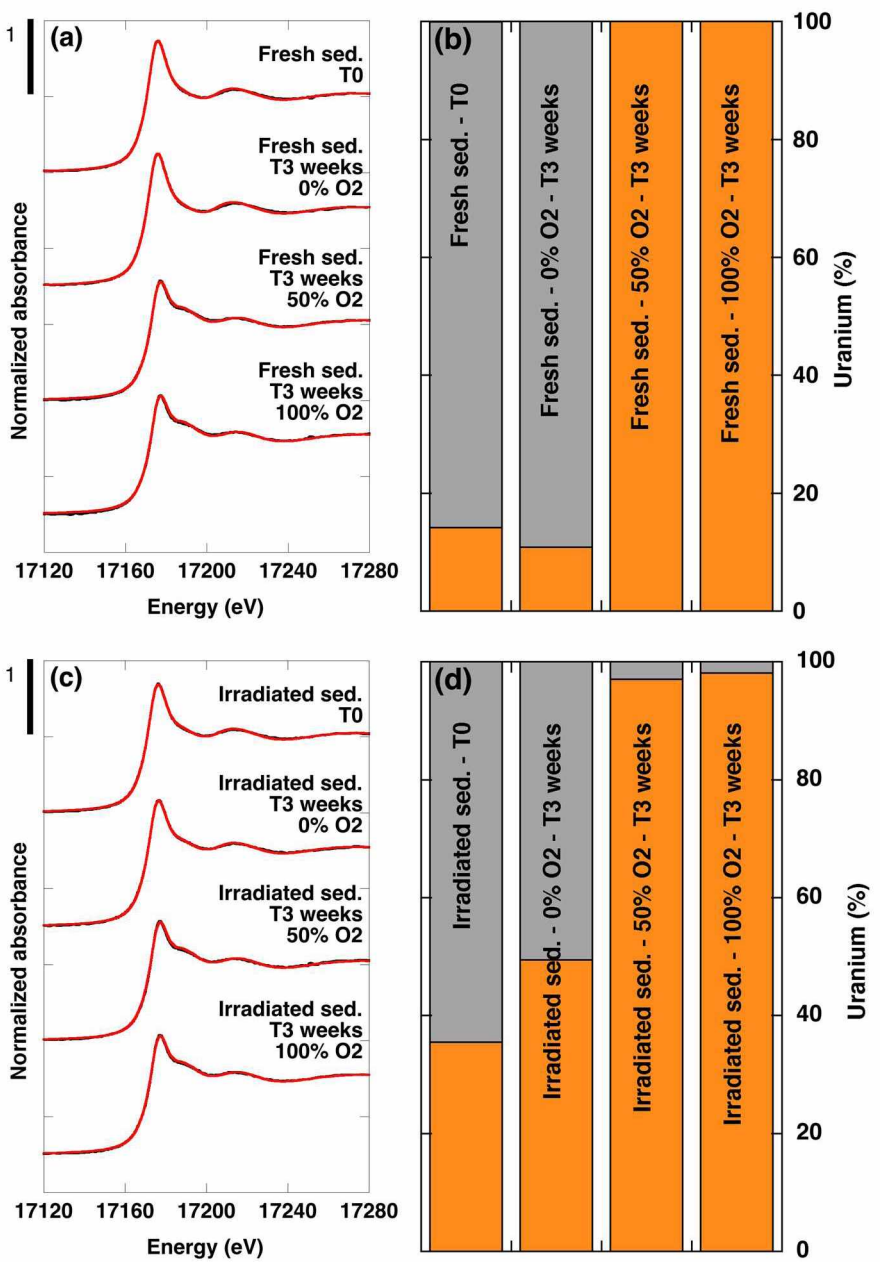

Fig. 4: U L_{III}-edge XANES experimental data (black) and fit (red) and the corresponding proportions of U(IV) (grey) and U(VI) (orange) for (a, b) fresh sediments and (c, d) irradiated sediments. XANES LC-LS fitting components are reported in Table S2.

In unreacted non-irradiated sediments (Figure 3a,b), U was mostly in the U(IV) form (~86% of total U) and remained in this reduced form (~89% of total U) after 3 weeks under anoxic conditions (i. e. *0% O_2*). In contrast, U was ~100% U(VI) after 3 weeks under hypoxic and fully oxic conditions (i. e. *50% O_2* and *100% O_2*) (Table S2).

The gamma-sterilization procedure was found to induce a partial oxidation of U, with U(IV) decreasing from ~86 to ~65% (Figure 3c,d). The redox state of U remained then unchanged after 3 weeks under reducing conditions. In contrast, both under *50%* and *100% O_2* conditions, U was fully oxidized after 3 weeks.

These results indicate that our hypoxic conditions (50% O_2) were sufficient to fully oxidize U(IV) to U(VI) in the lacustrine sediments studied. In order to determine the influence of solution chemistry on U remobilization, including especially the effect of bicarbonate ions, U aqueous speciation was calculated using thermodynamic equilibrium approach, as detailed in the following section.

3.3. Uranium aqueous speciation at the end of the incubations

The final distribution of dissolved U species (Figure 5, Tables S3, S4, S5) was calculated with the geochemical code Phreeqc [59] using the chemical composition of the aqueous phase at the end of each experiment (Figures 1, 2, 3, 5). Chemical reaction taken into account in our model are listed in (Table S3) together with corresponding thermodynamic equilibrium constants, as taken from WATEQ4F database [59]. According to these calculations, U was expected to be mainly in the form of aqueous U(VI)-carbonate complexes at the end of the *50% O_2* and *100% O_2* experiments, with UO_2CO_3 and, to a lesser extent, $UO_2(CO_3)_2^{2-}$ complexes as major species (Figure 5). This result is consistent with the well-known affinity of U(VI) for aqueous carbonate species, which results in the formation of a variety of soluble U(VI)-

carbonato complexes at near neutral and alkaline pH (Clark et al., 1995). A previous study on the same sediments indicated the importance of this process in U release under alkaline conditions (Seder-Colomina et al., 2018). For the *0% O_2* experiments, aqueous U was also calculated to be present as aqueous U(VI)-carbonate complexes, in the form of $CaUO_2(CO_3)_3^{2-}$ (71.9 and 45.2%) and, to a lesser extent, $UO_2(CO_3)_2^{2-}$ (7.7 and 30.6%) for non-irradiated and irradiated sediments, respectively (Figure 4). In these anoxic experiments, a minor fraction of dissolved U (11-18%) was calculated to be under the U(IV) form, complexed to dissolved organic matter (Figure 5). Moreover, 3 to 5% of U(VI) associated to humate was found for all the irradiated sediments. These results suggested an important role of U(VI) complexation by carbonates as a driver for U mobilization from the sediments, including in the anoxic incubation experiments.

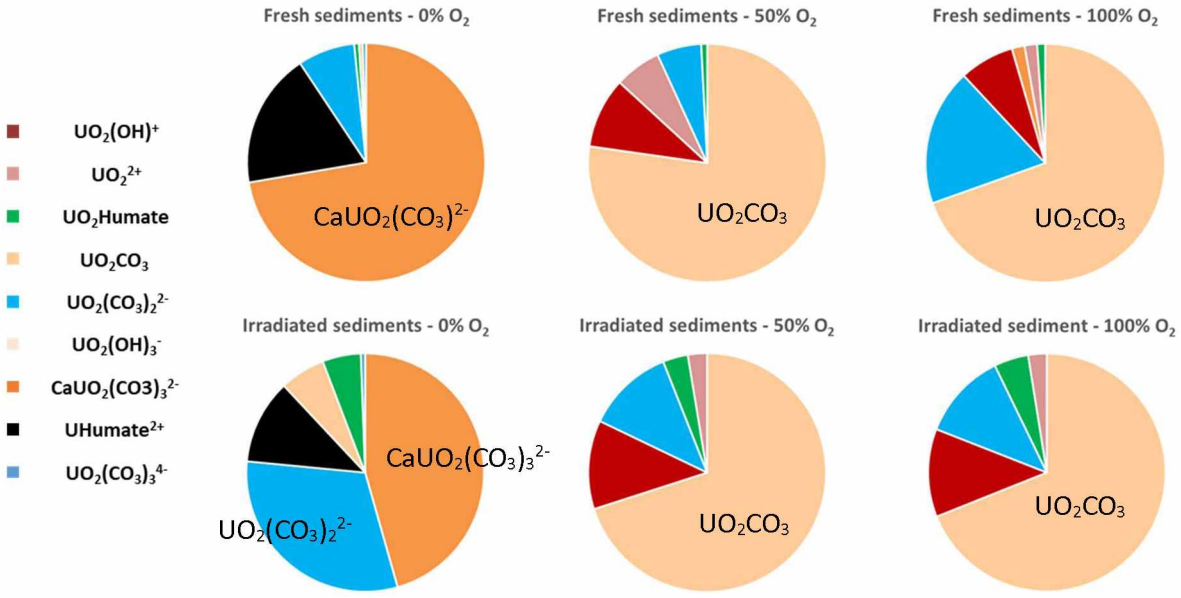

Fig. 5 Equilibrium calculations of dissolved uranium speciation at the end of each experiment. Calculation were conducted with Phreeqc [59] using the chemical composition of the aqueous phase at the end of each experiment (Table S4 and S5). Redox conditions were considered to be controlled by dissolved oxygen for the *50% O_2* and *100% O_2* experiments and by aqueous Fe^{2+} for the *0% O_2* experiments.

3.4. Evolution of microbial communities of the sediments in the incubation

Considering the global analysis of the dataset, NMDS plot revealed that both oxic conditions (*100% O_2* and *50% O_2* samples) exhibited the greatest sample variation and clustered closely together (Figure S5). A permutation test confirmed that the redox conditions of exposition explained most of the variance (R^2 of 0.96, *p*-value of 0.001). Most OTUs (1144 among 1214) are detected regardless of the experimental conditions (Figure 6A). Remaining OTUs are specific to oxygenation conditions. Few OTUs, which were not detected in initial sediments, were detected after 3 weeks incubation in controlled oxygen conditions.

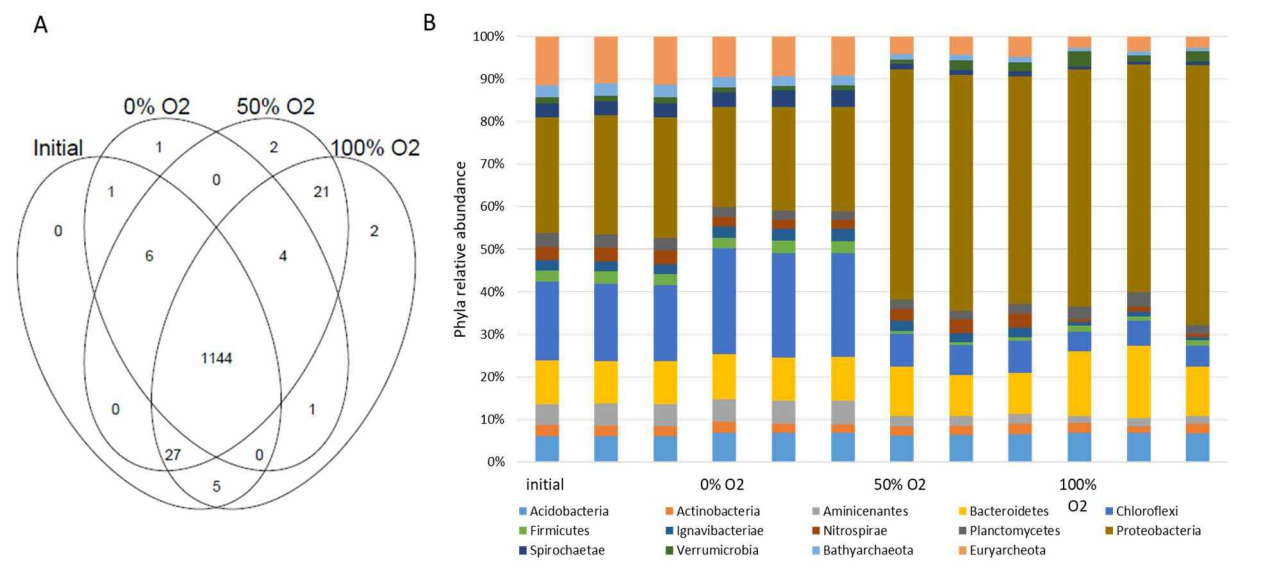

Fig. 6 A: Venn diagram of OTU repartition showing the overlap of the prokaryotic community for the initial sediments and after 3 weeks of incubation under different O_2 conditions (*100% O_2*, *50% O_2* and *0% O_2* samples). B: Relative abundance of OTUs at the phyla level for the initial sediments and after 3 weeks of incubation under different O_2 conditions. Phyla corresponding to more than 1% abundance are considered.

Relative abundances of phyla greater than 1% are close in the initial sediment and in sediment incubated in anoxia for 3 weeks. Likewise, close relative abundances are observed under oxic and hypoxic incubation conditions (Figure 6B). Proteobacteria are also favored

414 under oxic and hypoxic conditions, while the bacterial phyla *Chloroflexi*, *Firmicutes*
415 *Aminicenantes, Spirochaetes* are less abundant as well as the Archaea phyla of *Euryarcheota*
416 and *Bathyarcheota*. As expected, these results confirm that oxygenation is a strong structuring
417 factor of prokaryotic communities in our incubation conditions.

418 Since microaerophilic conditions were shown the most favourable conditions for decreasing
419 U remobilization from the lacustrine sediments, Figure 7 shows the 30 most abundant OTUs
420 after 3 weeks of incubation under hypoxic conditions (similar data for initial sediment, fully
421 oxic and anoxic conditions are given figure S6). OTU 4 corresponding to *Thiobacillus* is present
422 everywhere but dominates in oxic conditions. However, considering *50% O_2* incubation
423 condition, 3 OTUs appear specifically dominant in this condition. One (OTU 115) is affiliated
424 to Nitrosomodales (0.7379) and to Gallionellaceae (0.69) a family containing ferrous iron -
425 oxidizing bacteria [60-61], already noticed in prototype 19 in the network analysis. The second
426 (OTU 85) belongs to Hydrogenophilale order which contains only one family and two genus :
427 *Hydrogenophilus*, known as thermophile, but the existence of non thermophilic strains is
428 probable because DNA of *Hydrogenophilus thermoluteolus* was detected in ice core samples
429 [62], and *Thiobacillus* corresponding to sulphur oxidizing bacteria. The last one (OTU 29) is
430 affiliated to candidatus *Odyssella* genus, whose type species was described as an obligate
431 intracellular parasite of *Acanthamoeba sp.* [63], a group of amoeba forming cysts under anoxic
432 conditions, able of revival under oxygenated conditions [64] and sensitive to high oxygen
433 concentration[65].

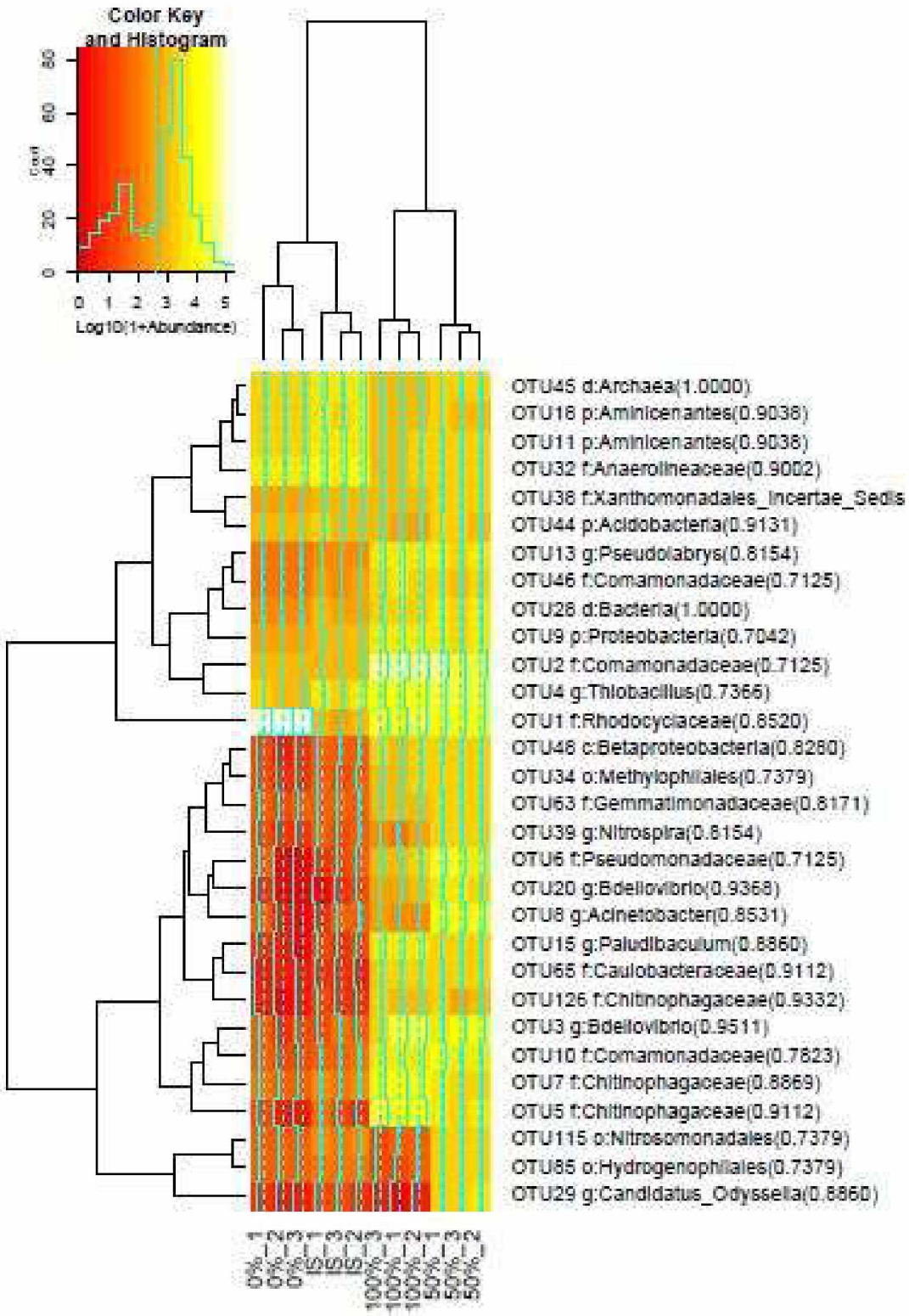

434

435 **Fig. 7** Heat map and hierarchical cluster analysis of log-transformed abundances of the 30 most
436 abundant OTUs (based on raw abundances under hypoxic conditions) after 3 weeks of
437 incubation. The dendrogram represents complete linkage clustering. Assignments after OTUs
438 numbers give the lowest taxonomic level associated with the OTU using the silva database k:
439 kingdom, p: phylum, o: order, f: family, s: genus_species. Values in brackets indicate sequence
440 similarity.
441

4. DISCUSSION

4.1. Effect of oxygenation and mechanism of U release

XANES results indicate that oxygenation lead to U(IV) oxidation to U(VI) in the solid phase and geochemical modelling indicated the formation of aqueous U(VI)-carbonato complexes leading to U release from the sediments. Moreover, even under anoxic conditions in which solid U(IV) was largely preserved, the formation of aqueous U(VI)-carbonato complexes shifts the U-redox couple equilibrium and also lead to U release[11,17,67]. In addition, the results of our biotic incubation experiments suggest that the oxygenation level of the incubation medium exerted a pivotal control on U mobilization rates from lake sediments, the lowest U release being observed under hypoxic conditions. In contrast, for abiotic experiments, the U release was higher and unaffected by the oxygenation level. The absence of an oxygenation effect for sterilized samples suggested that microbial activity could have been involved in the U removal under biotic conditions. The removal of U at the end of the hypoxic incubation was accompanied a drop in pH, alkalinity and dissolved Fe(II), which deserves to be interpreted under the light of the observed evolution of chemical and biological parameters during the incubation.

4.2. Effect of iron oxidation on alkalinity and pH

Aqueous U-carbonate complexes are favoured under alkaline conditions and are known to stabilize aqueous U(VI) against solid U(IV) species, which may thus facilitate the oxidation and dissolution of solid U(IV) species, even under anoxic conditions [6,11,17,66]. Conversely, the decrease in alkalinity and pH observed in our biotic *50% O_2* and *100% O_2* incubations (Figure 2a) may explain the limitation of U release (Figure 1) compared to more alkaline conditions

observed in our biotic *0%* O_2 incubations. This decrease in alkalinity observed under oxic and hypoxic conditions could be explained by the oxidation of aqueous Fe^{2+}, followed possibly by its precipitation as Fe^{3+} oxyhydroxides, as suggested by the removal of aqueous Fe^{2+} during these incubation experiments (Figure 3c). Ferric oxyhydroxide precipitation generates two H^+ ions for each oxidized Fe^{2+} ion and could thus explain the pH drop, while Fe^{2+} removal could explain the alkalinity drop (Figure 3c). Then, the acidification of the solution might have displaced the H_2CO_{3aq} / $HCO_3^-{}_{aq}$ equilibrium, which generated an excess of H_2CO_{3aq}. We suggest that CO_{2gas} degassing did then not reach equilibrium with atmosphere due to the use of air-permeable cotton stopper to close the Erlenmeyer flask, which have resulted in an accumulation of CO_2 in the lower section of the head-space and in solution, thus maintaining a low pH. Although not ideal, these conditions may be viewed as a semi-closed carbonate system that could however be considered as representative of confined conditions in a sub-surface storage site. These conditions may have limited aqueous complexation of U(VI) by bicarbonate ions and could also have favoured U adsorption onto ferric-oxyhydroxides, which deserves further discussion.

4.3. Effect of iron oxidation on U immobilization

The efficient removal of dissolved Fe(II) observed under biotic hypoxic conditions contrasts with the low Fe(II) removal observed for the other conditions, especially abiotic ones (Figure 3). Low oxygen concentrations such as those encountered under microaerophilic conditions are favourable to bacterial Fe(II) oxidation instead of fast and spontaneous abiotic reaction [67-68], which suggest that microbial process could be involved in the higher removal of Fe(II) under biotic hypoxic conditions (Figure 3c). Microbial Fe(II) oxidation is known to induce the formation of biogenic Fe(III) oxyhydroxides, frequently in the form of ferrihydrite and

493 lepidocrocite, with possible sequestration and/or nucleation of theses phases within the biofilm
494 [60,69-72]. Biogenic ferrihydrite is especially effective for sorbing U(VI) [73-76]and could thus have
495 contributed to the limitation of U release in our hypoxic biotic incubation experiments. It is
496 noteworthy, albeit abiotic oxidation of aqueous Fe^{2+} and ferric oxyhydroxides precipitation
497 likely occurred in our fully oxic biotic incubations, U was not removed from the solution, which
498 reinforce the possible role of microbial processes in U retention observed under hypoxic
499 conditions. Moreover, Fe(III) photoreduction previously identified in natural sediments [79] could
500 be another process which lead to the limited Fe(II) oxidation under fully oxidizing conditions.
501
502 **4.4 Influence of microbial communities on uranium mobility**
503
504 The observed microbial population dynamics suggested that hypoxic conditions have
505 favoured microaerophilic microbial populations. Indeed, these conditions revealed that OTU's
506 assigned to *Gallionellaceae* family were identified and described as a neutrophilic Fe oxidizer
507 family [60-61]. Two other OTU's identified under these conditions were known to be capable to i/
508 dissimilatory Fe(III) reduction (OTU 15 - *Paludibaculum* genus) (Figure 7) and related to ii/ a
509 Fe oxidizing family (OTU 115 - *Gallionellaceae* genus). Moreover, the predominance of
510 *Thiobacillus* genus under oxic conditions is an important result. This genus corresponds to
511 facultative anaerobiobligate chemolithotrophs using reduced sulphur compounds as energy
512 source. Indeed, acidophilic Fe oxidative bacteria were described in this genus, such as
513 *Thiobacillus ferrooxidans* and *Thiobacillus prosperus* but were then reclassified in other genera
514 [61,78]. Interestingly, *Thiobacillus denitrificans* is particularly notable for its ability to
515 oxidize sulfur and U compounds in a nitrate-dependent manner [79].
516 The particular abundance of this genus observed under microaerophilic conditions makes it
517 a potential actor of efficient of sulphur or Fe or U oxidation in these conditions. Moreover, the

specific abundance of OTU 115 identified could support our hypothesis of biologically mediated Fe oxidation that could explain the lower pH and the lower U mobilization observed under microaerophilic conditions. Its specific role needs to be further explored.

4.5 Effect of gamma-sterilization on uranium reactivity

Uranium release was observed to be higher in abiotic than in biotic conditions, with no influence of oxygenation conditions on the removal of U from the sterilized sediments. This behavior suggested a possible effect of the sterilization method as enhancing U mobility. Partial oxidation of U(IV) to U(VI) immediately after gamma-sterilization, under anoxic conditions, could be related to the formation of reactive oxygen species, for instance from water radiolysis, that could be able to oxidize U [17]. Although the actual mechanism and the identity of the U oxidized species remained not elucidated in the present study, irradiation prior to incubation appeared to favour the lability of U regardless the redox conditions (Figure 1b). However, solid U reoxidation was incomplete with minute amounts of residual U(IV), likely in the form of less reactive nanocrystalline U(IV)-phosphate[9] and/or as inaccessible U in metamictic zircon and monazite crystals identified previously in the sediments [9,10]. The increased U mobilization from the irradiated sediments could be explained by the higher U(VI) proportion than in the non-irradiated ones, at the start of the incubations (Figure 2). This mode of sterilization was also previously shown to favor U remobilization in oxidizing laboratory incubations [81], which was explained by the leaching of dead microbial cells and the release of DOC. In addition, the absence of microbial activity seems to have limited Fe^{2+} oxidation and removal of U under hypoxic conditions, by contrast with the higher Fe^{2+} removal (Figure 3) and pH drop (Figure 2) observed under biotic conditions, and which accompanied U removal from solution (Figure 1).

543 **4.6 Environmental implications**

544

545 The present study evidenced the potential role of microorganisms for minimizing the release
546 of U under oxidizing conditions that can be encountered after sediment dredging operations.
547 These results revealed that U sequestration in the sediment solid phase could be especially
548 favored under confined hypoxic conditions that enhance microbial Fe^{2+} oxidation. Indeed,
549 ferrous iron oxidation followed by ferric-oxyhydroxides precipitation lowers the pH and
550 alkalinity of the solution, which reduces the amount of available carbonate ligands available for
551 U(VI) mobilization. In addition, ferric-oxyhydroxides may sorb U(VI) and again limit its
552 mobility. Such a role of biogenic ferric-oxyhydroxides in U(VI) scavenging during reoxidation
553 of U(IV)-contaminated sediments is consistent with previous laboratory incubation conducted
554 on shallow groundwater sediments spiked with biogenic UO_2[74]. Here we show that biogenic
555 iron oxidation may limit U mobility during the reoxidation of genuine U-contaminated
556 sediments, carefully sampled under anoxic conditions in a mining-impacted lacustrine
557 environment. Hence, in our hypoxic experiment, dissolved U concentration ended up at only
558 3.6 $\mu g.L^{-1}$ after three weeks of incubation at a solid-solution ratio of 1:10. Under fully oxic or
559 anoxic conditions, U remobilization was higher but did not exceed 8.3 and 15 $\mu g.L^{-1}$,
560 respectively. This low U mobility contrast with the results of a previous study that have
561 addressed U remobilization from the same sediments in the presence of high bicarbonate
562 concentrations at pH value reaching ~9.5 [11]. In this latter study, the U release was up to 40 to
563 100 times higher at pH 8.5 to pH 9.5, due to U(VI) complexation to aqueous carbonate ions.
564 Our results show that oxygen can exert a strong control on the microbial community
565 structure, which can significantly influence the mobility of U. However, although oxygen is
566 generally assumed to favor U(IV) to U(VI) oxidation and release especially under acidic
567 conditions[82], our results suggest that more complex interactions occur under neutral pH

conditions, in which ferric iron is insoluble, which might be important to consider for evaluating contaminated sediments management practices. More precisely our results suggests that U(VI) mobilization from sediments could be limited by bacterial Fe(II) oxidizing activity under hypoxic conditions. Further research would be however needed to assess the efficiency of such a biogeochemical process under dynamic conditions constrained by seasonal fluxes of meteoric waters.

ACKNOWLEDGMENTS

This work was partially supported by the CNRS federator project Needs Environnement and by IRSN. We thank EDF and DREAL Rhône-Alpes Auvergne for having authorized access to the lake of Saint-Clément. The SSRL facilities are acknowledged for having provided beamtime. SSRL and SLAC are supported by the U.S. Department of Energy (DOE), Office of Science, Office of Basic Energy Sciences under Contract No. DE-AC02-76SF00515, the DOE Office of Biological & Environmental Research, and by the National Institutes of Health, National Institute of General Medical Sciences (including P41GM103393). Partial support was provided by the U.S. DOE BER and SBR program.

APPENDIX A. SUPPLEMENTARY DATA

REFERENCES

1. D. Brugge, L. J. de Lemos,, B. Oldmixon, Exposure pathways and health effects associated with chemical and radiological toxicity of natural uranium. Rev. Env. Health., 2005, 20, 177-194.
2. IRSN, MIMAUSA database website (https://mimausabdd.irsn.fr/), accessed 4 February 2022.

3. Y. Wang, M. Frutschi, E. Suvorova, V. Phrommavanh, M. Descostes, A. A. A. Osman, G. Geipel, R. Bernier-Latmani, Mobile uranium(IV)-bearing colloids in a mining-impacted wetland, Nat. Commun., 2013, 4, 2942.
4. C. Mikutta, P. Langner, J. R. Bargar, R. Kretzschmar, Tetra- and Hexavalent uranium forms bidendate-mononuclear complexes with particulate organic matter in a naturally uranium-enriched peatland, Environ. Sci. Technol., 2016, 50, 10465–10475.
5. A. Mangeret, P. Blanchart, G. Alcalde, X. Amet, C. Cazala, M.-O. Gallerand, An evidence of chemically and physically mediated migration of 238U and its daughter isotopes in the vicinity of a former uranium mine, J. Environ. Radioact., 2018, 195, 67–71.
6. L. Stetten, P. Blanchart, A. Mangeret, P. Lefebvre, P. Le Pape, J. Brest, P. Merrot, A. Julien, O. Proux, S. Webb, J. R. Bargar, C. Cazala, G. Morin, Redox Fluctuations and Organic Complexation Govern Uranium Redistribution from U(IV)-Phosphate Minerals in a Mining-Polluted Wetland Soil, Brittany, France, Environ. Sci. Technol., 2018a, 52, 13099–13109.
7. L. Stetten, P. Lefebvre, P. Le Pape, A. Mangeret, P. Blanchart, P. Merrot, J. Brest, A. Julien, J. R. Bargar, C. Cazala, G. Morin, Experimental redox transformations of uranium phosphate minerals and mononuclear species in a contaminated wetland, J. Hazard. Mater., 2020, 121362.
8. V. Noël, K. Boye, J. S. Lezama Pacheco, S. E. Bone, N. Janot, E. Cardarelli, K. Williams, J. R. Bargar, Redox Controls over the Stability of U(IV) in Floodplains of the Upper Colorado River Basin, Environ. Sci. Technol., 2017, 51, 10954–10964.
9. G. Morin, A. Mangeret, G. Othmane, L. Stetten, M. Seder-Colomina, J. Brest, G. Ona-Nguema, S. Bassot, C. Courbet, J. Guillevic, Mononuclear U (IV) complexes and ningyoite as major uranium species in lake sediments, Geochem. Perspect. Lett., 2016, 2, 95–105.
10. L. Stetten, A. Mangeret, J. Brest, M. Seder-Colomina, P. Le Pape, M. Ikogou, N. Zeyen, A. Thouvenot, A. Julien, G. Alcalde, J. L. Reyss, B. Bombled, C. Rabouille, L. Olivi, O. Proux, C. Cazala, G. Morin, Geochemical control on the reduction of U(VI) to mononuclear U(IV) species in lacustrine sediments, Geochim. Cosmochim. Acta, 2018b, 222, 171–186.
11. M. Seder-Colomina, A. Mangeret, L. Stetten, P. Merrot, O. Diez, A. Julien, E. Barker, A. Thouvenot, J. R. Bargar, C. Cazala, G. Morin, Carbonate Facilitated Mobilization of Uranium

620 from Lacustrine Sediments under Anoxic Conditions, Environ. Sci. Technol., 2018, 52, 9615–
621 9624.
622 12. H., Foerstendorf, K. Heim, A. Rossberg, The complexation of uranium(VI) and atmospherically
623 derived CO_2 at the ferrihydrite–water interface probed by time-resolved vibrational
624 spectroscopy. J. Colloid Interface Sci., 2012, 377, 299–306.
625 13. L. N. Moyes, R. H. Parkman, J. M. Charnock, D. J. Vaughan, F. R. Livens, C. R. Hughes, A.
626 Braithwaite, Uranium Uptake from Aqueous Solution by Interaction with Goethite,
627 Lepidocrocite, Muscovite, and Mackinawite: An X-ray Absorption Spectroscopy Study,
628 Environ. Sci. Technol., 2000, 34, 1062–1068.
629 14. D. Langmuir, Aqueous environmental Geochemistry, 1997, Prentice Hall Up. Saddle River NJ.
630 15. S. E. Bone, J. J. Dynes, J. Cliff, J. R. Bargar, Uranium(IV) adsorption by natural organic matter
631 in anoxic sediments, Proc. Natl. Acad. Sci. U. S. A., 2017, 114, 711.
632 16. G. Dublet, J. Lezama Pacheco, J. R. Bargar, S. Fendorf, N. Kumar, G. V. Lowry, G. E. Brown,
633 Partitioning of uranyl between ferrihydrite and humic substances at acidic and circum-neutral
634 pH, Geochim. Cosmochim. Acta, 2017, Acta 215, 122–140.
635 17. K.-U. Ulrich, E. S. Ilton, H. Veeramani, J. O. Sharp, R. Bernier-Latmani, E. J. Schofield, J. R.
636 Bargar, D. E. Giammar, Comparative dissolution kinetics of biogenic and chemogenic uraninite
637 under oxidizing conditions in the presence of carbonate. Geochim. Cosmochim. Acta, 2009, 73,
638 6065–6083.
639 18. D. E. Latta, K. M. Kemner, B. Mishra, M. I. Boyanov, Effects of calcium and phosphate on
640 uranium(IV) oxidation: Comparison between nanoparticulate uraninite and amorphous UIV–
641 phosphate. Geochim. Cosmochim. Acta, 2016, 174, 122–142.
642 19. Zhou P., Gu B. Extraction of oxidized and reduced forms of uranium from contaminated soils:
643 effect of carbonate concentration and pH. Environ. Sci and Technol., 2005, 39, 4435-4440.
644 20. L. Newsome, K. Morris, J. R. Lloyd, The biogeochemistry and bioremediation of uranium and
645 other priority radionuclides, Chem. Geol., 2014, 363, 164–184.
646 21. D. R. Lovley, E. J. Philips, Y. A., Gorby, E. R., Landa, E. R., Microbial reduction of uranium.
647 Nature, 1991, 350, 413-416.

22. R. Bernier-Latmani, H. Veeramani, E. D. Vecchia, P. Junier, J. S. Lezama-Pacheci, E. I. Suvorova, J. O. Sharp, N. S. Wigginton, J. R. Bargar, Non-uraninite products of microbial U(VI) reduction, Env. Sci. Technol., 2010, 44, 9456-9462.
23. D. R., Brookshaw, R. A. D. Pattrick, P. Bots, G. T. W. Law, J. R. Lloyd, J. F. W. Mosselmans, D. J. Vaughan, K. Dardenne, K. Morris, Redox interactions of Tc(VII), U(VI) and Np (V) with microbially reduced biotite and chlorite, Environ. Sci. Technol., 2015, 49, 13139-13148.
24. E. J. O'Loughlin, S. D. Kelly, R. E. Cook, R. Csencsits, K. M. Kemner, Reduction of uranium(VI) but mixed iron(II)/iron(III) hydroxide (green rust): formation of UO2 nanoparticles., Environ. Sci. Technol., 2003, 37, 721-727.
25. M. Ginder-Vogel, B. Stewart, S. Fendorf, Kinetic and mechanistic constraints on the oxidation of biogenic uraninite by ferrihydrite, Environ. Sci. Technol., 2010, 44, 163-169.
26. J. M. Senko, Y. Mohamed, T. A. Dewers, L. R. Krumholz, Role of Fe(III) minerals in nitrate-dependent microbial U(IV) oxidation, Environ. Sci. Technol., 2005, 39, 2529-2536.
27. M. J. Beazley, R. J. Martinez, P. A. Sobecky, S. M. Webb, M. Taillefert, Nonreductive biomineralization of uranium(VI) phosphate via microbial phosphatase activity in anaerobic conditions, Geomicrob. J., 2009, 26, 431-441.
28. I., Llorens, G. Untereiner, D. Jaillard, B. Gouget, V. Chapon, M. Carriere, Uranium interaction with two multi-resistant environmental bacteria: *cupriavidus metallidurans* CH34 and *rhodopseudomonas palustris,* Plos One, 2012, 7, e51873.
29. M. Kalin, W. N. Wheeler, G. Meinrath, The removal of uranium from mining waste water using algal/microbial biomass, J. Environ. Radioact., 2005, 78, 151–177.
30. M. Seder-Colomina, G. Morin, J. Brest, G. Ona-Nguema, N. Gordien, J.-J. Pernelle, D. Banerjee, O. Mathon, G. Esposito, E. D. van Hullebusch, Uranium(VI) Scavenging by Amorphous Iron Phosphate Encrusting Sphaerotilus natans Filaments, Environ. Sci. Technol., 2015, 49, 14065–14075.
31. F. G. Ferris, R. O. Hallberg, B. Lyvén, K. Pedersen, Retention of strontium, cesium, lead and uranium by bacterial iron oxides from a subterranean environment, Appl. Geochem., 2000, 15, 1035-1042.

676 32. I. A. Katsoyiannis, Carbonate effects and pH-dependence of uranium sorption onto
677 bacteriogenic iron oxides: kinetic and equilibrium studies. J Hazard. Mater., 2007, 139, 31-37.
678 33. M. Seder-Colomina, G. Morin, K. Benzerara, G. Ona-Nguema, J.-J. Pernelle, G. Esposito, E.
679 D. van Hullebusch, Sphaerotilus natans, a neutrophilic-iron related sheath-forming bacterium:
680 perspective for metal remediation strategies. Geomicrob. J., 2014, 31, 64-75.
681 34. M. L. Merroun, S. Selenska-Pobell, Bacterial interactions with uranium: an environmental
682 perspective. J. Contam. Hydrol., 2008, 102, 285-295.
683 35. U. K. Banala, N. P. I. Das, S. R. Toleti, Microbial interactions with uranium: towards an
684 effective bioremediation approach, Env. Technol. Innov., 2021, 21, 101254.
685 36. M. Bader, K. Müller, H. Foerstendorf, M. Schmidt, K. Simmons, J. S. Swanson, D. T. Reed, T.,
686 Stumpf, A. Cherkouk, Comparative analysis of uranium bioassociation with halophilic bacteria
687 and archaea, Plos One, 2018, 13, e0190953.
688 37. G. Radeva, A. Kenarova, V. Bachvarova, K. Flemming, I. Popov, D. Vassilev, S. Selenska-
689 Pobell, Phylogenetic diversity of archaea and the archaeal ammonia monooxygenase gene in
690 uranium mining-impacted locations in Bulgaria, Archaea, 2014, 196140.
691 38. J. A. Siles, R. Margesin, Abundance and Diversity of Bacterial, Archaeal, and Fungal
692 Communities Along an Altitudinal Gradient in Alpine Forest Soils: What Are the Driving
693 Factors? Microb. Ecol., 2016, 72, 207–220.
694 39. C. Reitschuler, K. Hofmann, P. Illmer, Abundances, diversity and seasonality of (non-
695 extremophilic) Archaea in Alpine freshwaters. Antonie Van Leeuwenhoek, 2016, 109, 855–
696 868.
697 40. K. M.Campbell, R. K. Kukkadapu, N. P. Qafoku, A. D. Peacock, E. Lesher, K H. Williams, J.
698 R. Bargar, M. J. Wilkins, L. Figueroa, J. Ranville, J. A. Davis, P. E. Long, Geochemical,
699 mineralogical and microbiological characteristics of sediment from a naturally reduced zone in
700 a uranium-contaminated aquifer. Appl. Geochem., 2012, 27, 1499–1511.
701 41. P. Lefebvre, A. Gourgiotis, A. Mangeret, P. Sabatier, P. Le Pape, O. Diez, P. Louvat, N.
702 Menguy, P. Merrot, C. Baya, M. Zebracki, P. Blanchart, E. Mallet, D. Jézéquel, J.-L. Reyss, J.

703 R. Bargar, J. Gaillardet, C. Cazala, G. Morin, Diagenetic formation of uranium-silica polymers
704 in lake sediments over 3,300 years, Proc. Nat. Acad. Sci. U. S. A., 2021, 118, 2021844118.
705 42. D. L. Stoliker, K. M. Campbell, P. M. Fox, D. M. Singer, N. Kaviani, M. Carey, N. Peck, J. R.
706 Bargar, D. B. Kent, J. A. Davis, Evaluating Chemical Extraction Techniques for the
707 Determination of Uranium Oxidation State in Reduced Aquifer Sediments, Environ. Sci.
708 Technol., 2013, 47, 9225–9232.
709 43. T. L. Bank, R. K. Kukkadapu, A. S. Madden, M. A. Ginder-Vogel, M. E. Baldwin, P. M. Jardine,
710 Effects of gamma-sterilization on the physico-chemical properties of natural sediments, Chem.
711 Geol., 2008, 251, 1-7.
712 44. G. Sarazin, G. Michard, F. Prevot, A rapid and accurate spectroscopic method for alkalinity
713 measurements in sea water samples, Water Res., 1999, 33, 290–294.
714 45. E. Viollier, P. Inglett, K. Hunter, A. Roychoudhury, P. Van Cappellen, The ferrozine method
715 revisited: Fe(II)/Fe(III) determination in natural waters. Appl. Geochem., 2000, 15, 785–790.
716 46. F. Mercier-Bion, R. Drot, J. J. Ehrhardt, J. Lambert, J. Roques, E. Simoni, X-ray photoreduction
717 of U(VI)-bearing compounds, Surf. Interface Anal., 2011, 43, 777–783.
718 47. B. Ravel, M. Newville, ATHENA, ARTEMIS, HEPHAESTUS: data analysis for X-ray
719 absorption spectroscopy using IFEFFIT, J. Synchro. Rad., 2005, 12, 537–541.
720 48. G. Morin, F. Juillot, C. Casiot, O. Bruneel, J.-C. Personné, F. Elbaz-Poulichet, M. Leblanc, P.
721 Ildefonse, G. Calas, Bacterial formation of tooeleite and mixed arsenic(III) or arsenic(V)-
722 iron(III) gels in the Carnoulès acid mine drainage, France. A XANES, XRD and SEM study,
723 Env. Sci. Technol., 2003, 37, 1705-1712.
724 49. M. O. Krause, J. H. Oliver, Natural widths of atomic K and L levels, K α X-ray lines and several
725 KLL Auger lines, J. Phys. Chem. Ref. Data, 1979, 8, 329-338.
726 50. J. G. Caporaso, C. L. Lauber, W. A. Walters, D. Berg-Lyons, C. A. Lozupone, P. J. Turnbaugh,
727 N Fierer, R. Knight, Global patterns of 16S rRNA diversity at a depth of millions of sequences
728 per sample, Proc. Natl Acad. Sci. U. S. A., 2011,108, 4516−4522.
729 51. S. Andrews, FastQC: a quality control tool for high throughput sequence data, 2010,
730 http://www.bioinformatics.babraham.ac.uk/projects/fastqc.

731 52. M. Martin, Cutadapt removes adapter sequences from high-throughput sequencing reads,
732 EMBnet J., 2014 17, 10-12.
733 53. R. C. Edgar, Search and clustering orders of magnitude faster than BLAST, Bioinformatics,
734 2010, 26, 2460-2461.
735 54. J. R. Cole, Q. Wang, J. A. Fish, B. Chai, D. M. McGarrell, Y. Sun, C. T. Brown, A. Porras-
736 Alfaro, C. R. Kuske, J. M. Tiedje, Ribosomal Database Project: data and tools for high
737 throughput rRNA analysis, Nucleic Acids Res., 2014, 42, D633-D642.
738 55. C. Lozupone, M. Lladser, D. Knights, J. Stombaugh, R. Knight, UniFrac: an effective distance
739 metric for microbial community comparison, ISME J, 2011, 5, 169–172.
740 56. P. J., McMurdie, S. Holmes, phyloseq: An R Package for Reproducible Interactive Analysis and
741 Graphics of Microbiome Census Data, PLoS One, 2013, 8, e61217.
742 57. A. Barberán, S. T. Bates, E. O. Casamayor, N. Fierer, Using network analysis to explore co-
743 occurrence patterns in soil microbial communities, ISME J., 2011, 6, 343.
744 58. G. R. Warnes, B. Bolker, L. Bonebakker, R. Gentleman, W. H. A. Liaw, T. Lumley, M.
745 Maechler, A. Magnusson, S. Moeller, M. Schwartz, gplots: various R programming tools for
746 plotting data. R package version, 2009, 2, 1.
747 59. D. L. Parkhurst, C. A. J. Appelo, Description and input of examples for PHREEQC Version 3
748 – A computer program for speciation, batch-reaction, one-dimensional transport, and inverse
749 geochemical calculations, 2016, U.S. Geological Survey Techniques and Methods, book 6,
750 chap. A43, 497 p., available only at http://pubs.usgs.gov/tm/06/a43/.
751 60. D. Emerson, E. J. Fleming, J. M. McBeth, Iron-oxidizing bacteria: an environmental and
752 genomic perspective, Annu. Rev. Microb., 2010, 64, 561-583
753 61. S., Hedrich, M. Schlömann, D. B. Johnson, The iron-oxidizing proteobacteria, Microbiology,
754 2011, 157, 1551–1564.
755 62. C. Lavire, P. Normand, I. Alekhina, S. Bulat, D. Prieur, J.-L. Birrien, P. Fournier, C. Hänni, J.-
756 R. Petit, Presence of Hydrogenophilus thermoluteolus DNA in accretion ice in the subglacial
757 Lake Vostok, Antarctica, assessed using rrs, cbb and hox, Env, Microb., 2006, 8, 2106-2114.

63. R. J. Birtles, T. J. Rowbotham, R. Michel, D. G. Pitcher, B. Lascola, S. Alexiou-Daniel, D. Raoult, Candidatus Odyssella thessalonicensis' gen. nov., sp. nov., an obligate intracellular parasite of Acanthamoeba species, Int. J. Syst. Evol. Microbiol., 2000, 1, 63-72.

64. N. A. Turner, G. A. Biagini, D. Lloyd, Anaerobiosis-induced differentiation of *Acanthamoeba castellanii*,. FEMS Microb. Lett., 1997, 157, 149-153.

65. I. Sifaoui, E. C. Yanes, M. Reyes-Batlle, R. L. Rodríguez-Expósito, I. L. Bazzocchi, I. A. Jiménez, J. E. Piñero, J. Lorenzo-Morales, L. K. Weaver, 2021, High oxygen concentrations inhibit Acanthamoeba spp, Parasitol. Res., 2021, 120, 3001-3005.

66. K.-U. Ulrich, A. Singh, E. J. Schofield, J. R. Bargar, H. Veeramani, J. O. Sharp, R. Bernier-Latmani, D. E. Giammar, Dissolution of biogenic and synthetic UO_2 under varied reducing conditions, Environ. Sci. Technol., 2008, 42, 5600-5606.

67. G. K., Druschel, D. Emerson, R. Sutka, P. Suchecki, G. W. Luther III, Low-oxygen and chemical kinetic constraints on the geochemical niche of neutrophilic iron(II) oxidizing microorganisms, Geochim. Cosmochim. Acta., 2008, 72, 3358-3370.

68. S. Vollrath, T. Behrens, P. van Cappelen,. Oxygen dependency of neutrophilic Fe(II) oxidation by *Leptothrix* differs from abiotic reaction, Geomicrob. J., 2012, 29, 550-560.

69. R. M. Cornell, U. Schwertmann,. The iron oxides: structure, properties, reactions, occurences and uses, 2003, John Wiley & Sons.

70. C. Hohmann G. Morin, G. Ona-Nguema J. M. Guigner, G. E., Brown Jr, A. Kappler, Molecular-level modes of As binding to Fe(III) (oxyhydr)oxides precipitated by the anaerobic nitrate-reducing Fe(II)-oxidizing Acidovorax sp. strain BoFeN1, Geochimica et Cosmochimica Acta, 2011, 75, 4699-4712.

71. A. Voegelin, R. Kaegi, J. Frommer, D. Vantelon, S. J. Hug, Effect of phosphate, silicate and Ca on Fe(III) precipitates formed in aerated Fe(II)- and As(III)-containing water studied by X-ray absorption spectroscopy, Geochim. Cosmochim. Acta., 2010, 74, 164-186.

72. A.-C. Senn, .R. Kaegi, S. J. Hug, K. G. Hering, S. Mangold, A. Voegelin, Compositon and structure of Fe(III)-precipitates formed by Fe(II) oxidation in water at near-neutral pH:

785 interdependent effects of phosphate, silicate and Ca, Geochim. Cosmochim. Acta, 2015, 162,
786 220-246.
787 73. L. Zhong, C. Liu, J. M. Zachara, D. W. Kennedy, J. E. Szecsody, B. Wood, Oxidative
788 remobilization of biogenic uranium(IV) precipitates: effects on iron(II) and pH, J. Environ.
789 Qual., 2005, 34, 1763-1771.
790 74. E. Liger, L. Charlet, P. van Cappellen, Surface catalysis of uranium(VI) reduction by iron(II),
791 Geochim. Cosmochim. Acta, 1999, 63, 2939-2955.
792 75. D. D. Boland, R. N. Collins, T. E. Payne, T. D. Waite, Effect of amorphous Fe(III) oxide
793 transformation on the Fe(II)-mediated reduction of U(VI). Env. Sci. Technol., 2011 45, 1327-
794 1333.
795 76. E. Krawczyk-Barsch, A. C. Scheinost, A. Rossberg, K. Muller, F. Bok, L. Hallbeck, J. Lehrich,
796 K. Schmeide Uranium and neptunium retention mechanisms in Gallionella
797 ferruginea/ferrihydrite systems for remediation purposes, Env. Sci. Pollut. Res., 2020, 28,
798 18342-18353.
799 77. I. S. Kulichevskaya, N. E. Suzina, W. I. C. Rijpstra, J. S. S. Damsté, S. N. Dedysh,
800 Paludibaculum fermentans gen. nov., sp. nov., a facultative anaerobe capable of dissimilatory
801 iron reduction from subdivision 3 of the Acidobacteria. Int. J. Syst. Evol. Microbiol., 2014, 64,
802 2857–2864.
803 78. J. Pablo Cárdenas, R. Ortiz, P. R., Norris, E. Watkin, D. S. Holmes, Reclassification of
804 'Thiobacillus prosperus' Huber and Stetter 1989 as Acidihalobacter prosperus gen. nov., sp.
805 nov., a member of the family Ectothiorhodospiraceae, Int. J. Syst. Evol. Microbiol, 2015, 65,
806 3641–3644.
807 79. Lueder U., Jørgensen B. B., Kappler A., Schmidt C. (2020) Fe(III) photoreduction producing
808 Fe_{aq}^{2+} in oxic freshwater sediment. Environ. Sci. Technol., 2020, 54, 862-869.
809 80. H. Beller, P. Zhou, T. Legler, A. Chakicherla, S. Kane, T. Letain, P. O'Day, Genome-enabled
810 studies of anaerobic, nitrate-dependent iron oxidation in the chemolithoautotrophic bacterium
811 Thiobacillus denitrificans, Front. Microbiol., 2013, 4, 249.

81. J. Schaller, A. Weiske, E. G. Dudel, Effects of gamma-sterilization on DOC, uranium and arsenic remobilization from organic and microbial rich stream sediment, Chem. Geol., 2011, 409, 3211-3214.

82. Lee, JU (Lee, JU) ; Kim, SM (Kim, SM) ; Kim, KW (Kim, KW) ; Kim, IS (Kim, IS) Microbial removal of uranium in uranium-bearing black shale. Chemosphere, 2005, 59, 147-154.